Scoping the Enantioselective Desymmetrization of a Poorly Water-Soluble Diester by Recombinant Pig Liver Esterase

Meissner, Murray P.; Süss, Philipp; Brundiek, Henrike; Woodley, John M.; von Langermann, Jan

Published in:
Organic Process Research And Development

Link to article, DOI:
10.1021/acs.oprd.8b00277

Publication date:
2018

Document Version
Peer reviewed version

Full Paper

Scoping the Enantioselective Desymmetrization of a Poorly Water-Soluble Diester by Recombinant Pig Liver Esterase

Murray P. Meissner, Philipp Süss, Henrike Brundiek, John M. Woodley, and Jan von Langermann

Org. Process Res. Dev., **Just Accepted Manuscript** • DOI: 10.1021/acs.oprd.8b00277 • Publication Date (Web): 16 Oct 2018

Scoping the Enantioselective Desymmetrization of a Poorly Water-Soluble Diester by Recombinant Pig Liver Esterase

Murray P. Meissner,[θ,β] Philipp Süss,[§] Henrike Brundiek,[§] John M. Woodley,[,θ] Jan von Langermann[*,†]*

[θ]Technical University of Denmark (DTU), Department of Chemical and Biochemical Engineering, Søltofts Plads, Building 229, 2800 Lyngby, Denmark

[β]Oxford Biotrans Ltd., 127 Olympic Avenue, Milton Park, OX14 4SA, United Kingdom

[§]Enzymicals AG, Walther-Rathenau-Str. 49a, 17489 Greifswald, Germany

[†]University of Rostock, Institute of Chemistry, Biocatalytic Synthesis Group, Albert-Einstein-Str. 3a, 18059 Rostock, Germany

Corresponding Authors

jw@kt.dtu.dk (John M. Woodley) and jan.langermann@uni-rostock.de (Jan von Langermann)

ABSTRACT. Previously, the biocatalytic desymmetrization of dimethyl cyclohex-4-ene-*cis*-1,2-dicarboxylate to (1*S*,2*R*)-1-(methoxycarbonyl)cyclohex-4-ene-2-carboxylic acid, an important intermediate towards the synthesis of biologically active molecules, had been well-characterized in terms of pH and temperature optima and several aspects of process performance. Eventually this promising reaction could convert 200 mM (40 $g \cdot L^{-1}$) of substrate with > 99.5% e.e. using the recombinant pig liver esterase, ECS-PLE06, at a scale of 8.8 L. However, the precise influence of substrate concentration and the poorly water-soluble nature of the substrate (approximately 60 mM in water at 25 °C for structurally similar dimethyl 1,4-cyclohexanedicarboxylate) remained elusive. Therefore, this work focuses on using a recently published methodology based on reaction trajectory analysis to identify mass transfer limitations in this reaction. With the constraints of mass transfer on space-time yield considered, it was possible to evaluate and improve biocatalyst yield (mass of product per mass of biocatalyst) through the use of higher substrate concentrations. Ultimately the complete conversion of approximately 75 $g \cdot L^{-1}$ substrate was achieved in 3.65 h yielding an excellent productivity of 20 $g \cdot L^{-1} \cdot h^{-1}$ with a biocatalyst yield of 4.36 $g \cdot g_{biocat}^{-1}$. This work also highlights the simplicity of applying a reaction trajectory analysis methodology, importance of scale during reaction characterizations and identifies future directions for reaction improvement to address substrate supply and product inhibition/deactivation.

KEYWORDS. Biocatalysis; recombinant Pig Liver Esterase (PLE); Reaction Scoping; Kinetic Characterizations; Substrate Mass Transfer

TOC-figure

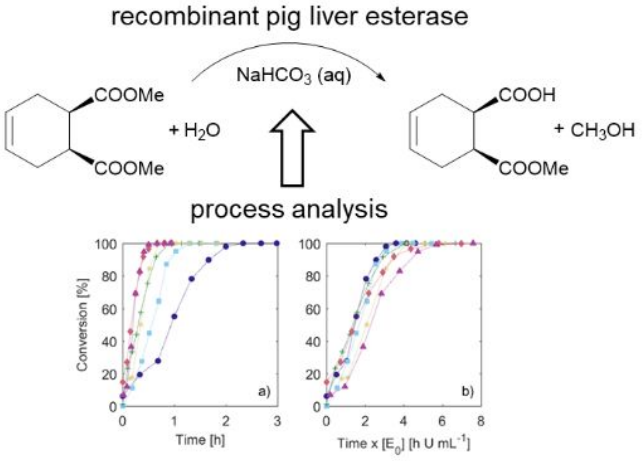
recombinant pig liver esterase
NaHCO3 (aq)
COOMe
COOMe
+ H2O
COOH
COOMe
+ CH3OH
process analysis
Conversion [%]
Time [h]
a)
Time x [E0] [h U mL-1]
b)

Introduction

Biocatalysis has become an established branch of chemistry in its own right resulting from the excellent stereo-, regio- and enantioselectivity of biocatalysts even under mild reaction conditions.[1,2] Consequentially, biocatalysts can realize sustainable manufacturing processes, satisfying 10 of the 12 principles of green chemistry: waste prevention and high atom efficiency (avoiding the formation of by-products) through their high selectivity, less hazardous syntheses, safer solvents (most often carried out in water), and low energy demand due to their operation under mild process conditions, their origin from renewable sugar feedstocks through fermentation, avoidance of derivatization, their nature as catalysts and not stoichiometric reagents, the ability to apply real-time process analytics to prevent waste, and most importantly, their inherent safety.[3] Additionally, these traits frequently (although not always) infer better process economics. Finally, biocatalysts can be further improved by protein engineering, offering an additional degree of freedom towards process design. Such improvements are gained through tailoring the amino acid sequences of enzymes to enhance stability, activity or selectivity.[4] Indeed, numerous biocatalytic processes have been successfully commissioned to date, using these approaches.[5-7]

Conventional catalysis is most often performed in homogeneous gas-phase reactors or organic solvents, where reaction scale-up is often dependent on adequate heat transfer and appropriate reactor design. For biocatalysis, under mild conditions (ambient temperature, near neutral pH and in aqueous-based media), this is less relevant. Instead, the conditions of the reaction become important and biocatalytic reaction performance can be estimated (or "scoped") using a standard set of process performance measures (metrics).[8] These metrics may be benchmarked against industrial requirements, while the importance and value of each respective metric may differ depending on the value of the product and target market. It is advantageous to be able to quantify

these metrics at a scale as small as possible, in order to allow fast and efficient process evaluation using the smallest possible amounts of (often expensive) materials. However, it turns out that in many cases these metrics do not scale well. Understanding these limitations of scale-up for biocatalysis helps address them during process development.

A major reason for performance changes across scales is due to substrate mass transfer limitations. It is well known that enzymes require at least some water to be present in their environment to be active.[9] Since organic substrates and products of synthetic interest are frequently poorly water-soluble, this results in mass transfer limitations.[10] This applies also to gas-liquid systems, such as the important enzyme-catalyzed oxidations[11], due to the particularly low water-solubility of oxygen. Interestingly, the scale-dependence of gas-liquid mass transfer is different from liquid-liquid mass transfer (see Table 1). Mixing is a function of power input, which can vary significantly with scale.[12] More specifically, it is easier to thoroughly mix a smaller volume to achieve good dispersion (high power input per unit volume) than it is to mix a large volume. As dispersion increases, so does the specific interfacial area (m^{-1}) of the second phase component (smaller gas bubbles or liquid droplets), which leads to improved mass transfer. However, when considering gas-liquid mass transfer, an even greater influence is the increased gas hold-up at larger scales, allowing an increase in overall volumetric mass transfer coefficient (k_La).[13] In contrast, liquid-liquid systems are not affected by hold-up because the volumetric component remains in the reaction volume unlike gases, which pass through a reactor. Furthermore, liquid-liquid systems have the ability to be emulsified by adding surfactants resulting in a homogeneous medium, which being independent of mixing thereby makes them scale-independent. While solid-liquid systems are not in focus in this work, similar parallels can be drawn, although they are less

dependent on mixing to ensure a high interfacial area and are rather influenced more by initial particle size.

Table 1. Effect of scale on gas-liquid and liquid-liquid mass transfer.

	Gas-Liquid Mass Transfer		Liquid-Liquid Mass transfer	
	Dispersion (i.e. bubble size)	Hold-up [a]	Dispersion (i.e. droplet size / coalescence) [b]	Hold-up
Small-scale	↑	↓↓	↑	N/A
Large-scale	↓	↑↑	↓	N/A
[a] The extent of effect of hold-up on mass transfer is more or less pronounced for plug-flow or well-mixed regimes, respectively.[12]				
[b] Stable emulsions create a homogeneous medium that will be independent of mixing.				

It is therefore important to consider the scale at which reaction assessments are performed because some mass transfer limited reactions (e.g. gas-liquid systems) will not proceed at the same rate at a small-scale as at larger scales. The most important metrics to evaluate under these circumstances are the biocatalyst yield and product concentration. These indicate if the catalyst is sufficiently efficient and if enough product can be generated in a reasonable amount of time. Time-course measurements are an effective means to assess reaction performance and gauge these metrics. Recently, a method making use of comparing normalized time-course measurements (or reaction trajectories) under different experimental conditions was used to distinguish mass transfer limitations from other kinetic effects (e.g. enzyme stability, substrate affinity or intrinsic activity).[14] Additionally, the mechanism of enzyme deactivation or potential substrate/product inhibition can also be identified using such time-course progressions.[14-17] Time-course progressions also give indication of the expected productivity of a reaction, and already at this

stage, reactions that proceed too slowly may be earmarked for improvement. Naturally, only metrics assessed at a larger scale can be considered true process metrics, although understanding how to gauge a reflection of the metrics at smaller scales is invaluable to the effectiveness of process development.

In this work, a recently published procedure of reaction scoping for biocatalysis[14] was applied to the enantioselective desymmetrization of dimethyl cyclohex-4-ene-*cis*-1,2-dicarboxylate (**1**) to (1*S*,2*R*)-1-(methoxycarbonyl)cyclohex-4-ene-2-carboxylic acid (**2**) catalyzed by recombinant pig liver esterase (rPLE; ECS-PLE06; Scheme 1).[18] The monoester product of this reaction is of value as a pharmaceutical intermediate towards the synthesis of biologically active molecules[19] (some examples are shown in Scheme 1)[20], the antibiotic plantencin[21] as well as some active pharmaceutical ingredients in treatments towards HIV[22] and cytomegalovirus (Herpes)[23]. Previously, this reaction and enzyme were characterized in terms of pH and temperature optima as well as reaction performance.[18,24,25] A simple method of pH control was implemented that made use of inexpensive sodium bicarbonate degradation in the presence of the carboxylic acid product **2**, thereafter forming CO_2 and passing from the reaction medium. This was found to be more effective than conventional titration of base to control the pH. In addition, the pH remains stable within non-saturated bicarbonate solutions. Eventually this promising reaction showed adequate performance to convert substrate concentrations of 200 mM (40 $g \cdot L^{-1}$) with an enantiomeric excess of > 99.5%.[18] However, this reaction performance came from a series of improvised experiments and the bottleneck towards large-scale production was not determined. On this basis, we argued that it would be valuable to perform a bottleneck identification using reaction trajectory analysis[14] to determine the major process limitation. Using time-course measurements in this way we argued it would be possible to distinguish the dominating bottleneck to the required performance of ECS-

PLE06 under given conditions: either enzyme kinetics, enzyme stability or, more likely, substrate mass transfer. With this limitation identified, the reaction could be further up-scaled and its suitability for process implementation assessed.

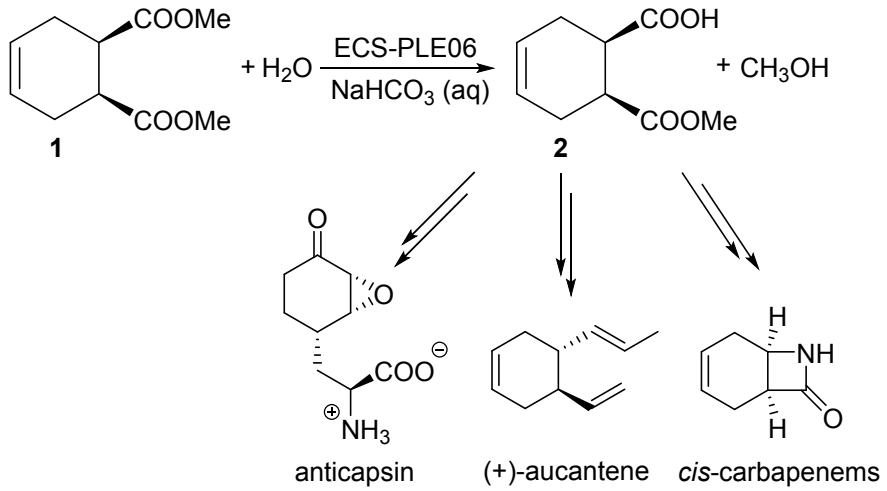

Scheme 1. Desymmetrization of diester **1** to (1*S*,2*R*)-monoester **2** catalyzed by recombinant pig liver esterase (ECS-PLE06).

Results and Discussion

Understanding the influence of the poorly water-soluble substrate on this system initially required a series of time-course experiments with varying enzyme concentrations (expressed as dosed activities) to identify potential mass transfer limitations. With this limitation on reaction rate considered, process performance metrics were assessed. Further scale-up was then considered with the goal of maximizing product concentration.

The first step in this systematic procedure was to elucidate the major reaction limitation by varying enzyme loadings at a fixed, moderate substrate dose. Figure 1a shows representative time-course progressions at different enzyme doses at a fixed substrate concentration of 80 mM. Normalizing the time axis by the varied parameter (enzyme activity) reveals that the reaction becomes substrate mass transfer limited at enzyme doses above ca. 6 $U \cdot mL^{-1}$, since the reaction

trajectories diverge (Figure 1b). Interestingly, the product was found to have a beneficial effect by better dispersing the substrate in the reaction medium since it acts as an emulsifier. Likewise, methanol was also formed as a by-product, which would (at higher concentrations) help improve substrate solubility in the medium (and thereby reduce mass transfer limitations). The slight improvement in reaction rate due to these factors can be observed after initial product formation, especially at the lowest enzyme doses.

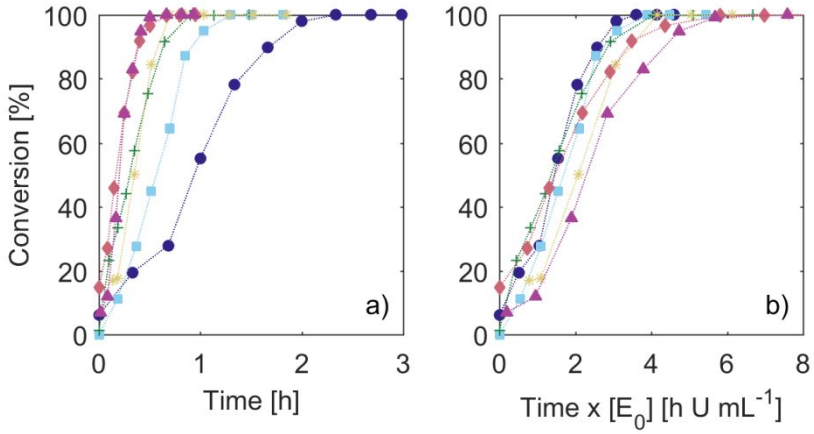

Figure 1. (a) Conversion as a function of time for the ECS-PLE06 catalyzed reaction of 80 mM diester **1** to monoester **2** using 40 mL saturated $NaHCO_3$ as a buffer (pH 8.15) at 40 °C in a stirred round bottom flask (left). (b) Data replotted with the x-axis normalized by enzyme concentration to reveal the major process limitation (right). ECS-PLE06 concentrations, $[E_0]$, were varied as follows: ● – 1.54 U·mL^{-1}, ■ – 2.99 U·mL^{-1}, + – 4.50 U·mL^{-1}, * – 5.94 U·mL^{-1}, ♦ – 8.72 U·mL^{-1}, ▲ – 11.37 U·mL^{-1}.

Figure 2 is a plot of space-time yield and biocatalyst yield as a function of enzyme activity. According to Figure 2, the upper limit of productivity due to substrate mass transfer limitations is 21 g·L^{-1}·h^{-1}. Clearly, the expected linear response of space-time yield to enzyme activity no longer holds beyond this point, indicating a non-enzyme related limitation. On the other hand, biocatalyst

yield appears to improve at lower enzyme concentrations because the same amount of substrate is still converted, even though the reactions take longer. Another way of improving the biocatalyst yield is to increase the substrate loading thereby converting more substrate with the same amount of enzyme. In this way, a better reflection of biocatalyst yield is obtained because, in reality, industrial processes should operate with the highest possible space-time yield in order to afford cost-effective processes (shorter batches and smaller reaction volumes). However, the most representative biocatalyst yield should still be evaluated under conditions where the reaction is not kinetically limited. This is especially important to consider in cases such as this, which are limited by liquid-liquid mass transfer.

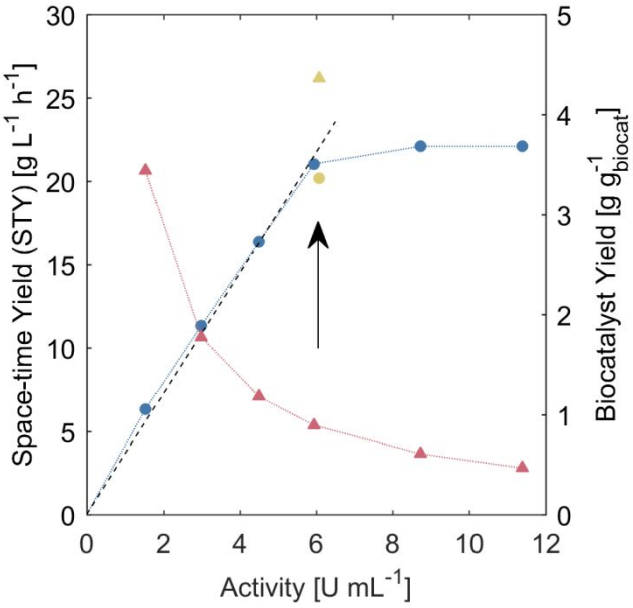

Figure 2. Space-time yield (STY; blue ●) and biocatalyst yield (red ▲) as a function of rPLE dose (presented as activity) after the full conversion of 80 mM substrate. The dashed line indicates linearity through the origin. Data in yellow are those obtained after the full conversion of 400 mM substrate.

Hence, the substrate concentration was increased 5-fold (400 mM) and an enzyme dose of 6 $U \cdot mL^{-1}$ was maintained because mass transfer limitations only occurred at higher enzyme concentrations. Full conversion and no kinetic limitations were observed at this higher substrate concentration, which was confirmed by the overlap of trajectories on a normalized time axis plot (Figure 3). The resultant 4.9-fold improvement in biocatalyst yield from 0.89 to 4.36 $g \cdot g_{biocat}^{-1}$ at an almost identical maximum space-time yield is shown in Figure 2.

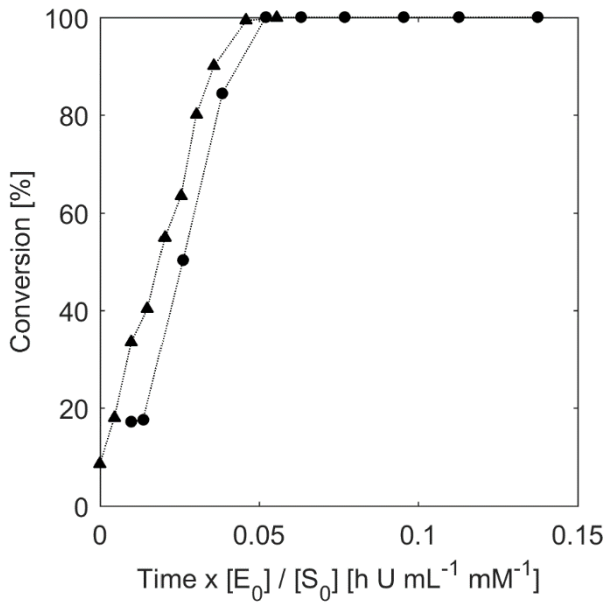

Figure 3. Reaction with 80 mM substrate (●) and 400 mM substrate (▲) in 40 mL saturated $NaHCO_3$ buffer (pH 8.15) at 40 °C both with an enzyme dose of 6 U mL^{-1} on a normalized time-axis plot.

In order to investigate the potential of further increasing substrate concentration, it was necessary to marginally increase the scale of reaction by operating in a 250 mL stirred tank reactor. At this scale, better control and measurement of the reaction environment was made possible through defined stirring, temperature and pH control. Substrate concentrations greater than 500 mM caused the enzyme to agglomerate and denature. Therefore, three 400 mM batch doses of **1** were supplied

at 3 h intervals in a fed-batch manner to mimic the previous reaction profiles observed at smaller scale. Nevertheless, full conversion was not reached even after 24 h (data not shown). In order to rule out potential substrate inhibition caused by too high single substrate concentration doses, a constant feed of substrate at 5.81 $g \cdot h^{-1}$ was instead supplied to the reactor by use of a syringe pump. This would hypothetically result in a calculated 1.19 M (225 $g \cdot L^{-1}$) product and a space-time yield of 22.0 $g \cdot L^{-1} \cdot h^{-1}$ in a 9 h reaction, assuming the reaction is not limited. However, during a fed-batch reaction, product formation ceased after 7 h, after which substrate accumulated at a rate equal to that of the pump feed rate (Figure 4a). Since the mass balance of substrate and product closed throughout the reaction, this result indicated that indeed the reaction had stopped after 400 mM product formation (Figure 4b). We postulated therefore that either enzyme stability or product inhibition could be the cause. In order to confirm this, the end-point reaction medium was dosed with a fresh 6 $U \cdot mL^{-1}$ of ECS-PLE06 and left to incubate at 40 °C for 48 h. Conversion was only marginally improved by approximately 10% (data not shown) indicating that product inhibition or product induced deactivation was the most likely cause of activity loss.

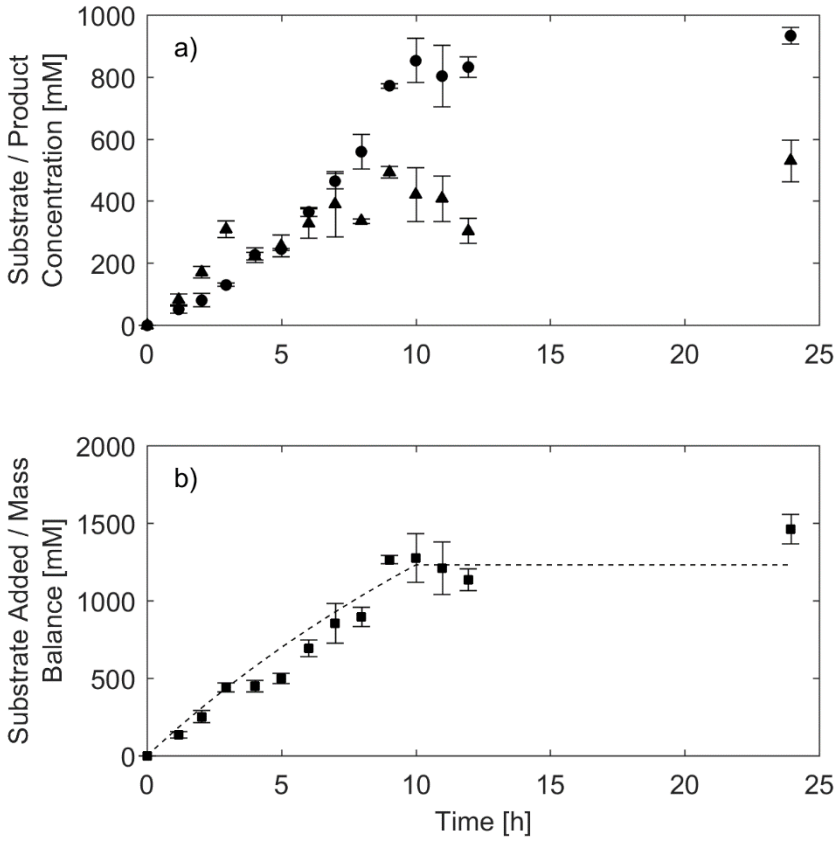

Figure 4. (a) Fed-batch conversion of 1.2 M diester **1** (●) to monoester **2** (▲) in a 250 mL (end volume) stirred tank reactor. pH was maintained with saturated $NaHCO_3$ buffer (pH 8.15) at 40 °C and included an enzyme dose of 6 $U \cdot mL^{-1}$ (above). (b) Mass balance corresponding to the sum of substrate and product in the reaction medium (●) the actual fed-batch rate of substrate supply to the reactor by a syringe pump (below). Error bars reflect 95% confidence intervals (n = 3).

In order to test this further, the time-dependent stability of ECS-PLE06 was evaluated with respect to temperature (40 °C), high buffer strength solutions (saturated $NaHCO_3$), and by-product methanol concentrations of up to 5% (v/v) (corresponding to a high molar concentration of ca. 1.3 M; Figure 5). ECS-PLE06 showed a negligible activity loss after 24 h in the presence of all environmental factors. Furthermore, the enzyme gained activity whilst being incubated in $NaHCO_3$

buffer and methanol, which might point towards an affinity of ECS-PLE06 for strongly buffered environments containing methanol. This confirmed that the remaining limitation to be addressed was product inhibition or product induced deactivation.

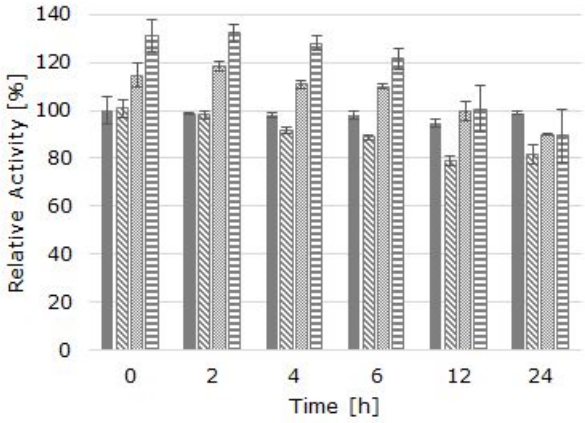

Figure 5. Stability of ECS-PLE06 as a function of time at room temperature in 50 mM phosphate buffer at pH 7.5 (control, solid bars), at 40 °C in 50 mM phosphate buffer (pH 7.5; diagonal striped bars), at 40 °C in saturated $NaHCO_3$ buffer (1.14 M, pH 8.15; opaque bars), and with 5% (v/v) methanol (~1.3 M) at 40 °C in saturated $NaHCO_3$ buffer (horizontal striped bars). Error bars reflect 95% confidence intervals ($n = 4$).

In situ product removal (ISPR) techniques could potentially be applied to address product inhibition/deactivation. The method of reactive crystallization would be particularly interesting because it could be implemented through the selection of an appropriate metal bicarbonate salt. In this way, the charged product anion could potentially precipitate from solution when bound to the metal cation without negatively affecting enzyme performance. Furthermore, the bicarbonate ion would also help buffer the pH during reaction presenting a potent 'self-healing' system. This method of reactive crystallization ISPR was recently demonstrated with a transaminase reaction to improve the thermodynamic equilibrium to favor product formation.[26] Ultimately, product in

the form of solid precipitates resulted in a product concentration in excess of 1 M. For the case of the rPLE reaction, two-liquid phase ISPR approaches would not be feasible because the substrate, being hydrophobic, would partition more strongly than the product into an organic phase. Instead, further focus could be made towards more expensive ISPR methods such as selective ion exchange resins[27,28] or charged membranes[29]. Another possibility could be to remove the product in an external loop through pH swing (precipitation) or cooling crystallization, although this is less likely to be feasible since the excess bicarbonate would need to be removed and such a system would also require a means to retain the biocatalyst from the harsh conditions in the external loop.[30,31] The reaction itself might be also further improved by the use of specific ionic liquids as additives.[32]

Conclusions

Through the application of a standardized methodology relying on reaction trajectory analysis, it was concluded that the reaction was limited by mass transfer. This was due to the low solubility of substrate in the water-based medium. ECS-PLE06 is a robust enzyme that is highly thermostable and tolerant towards solvents[25], therefore mass transfer limits could still potentially be reduced by increasing temperature or adding water-miscible co-solvents to this system to improve substrate solubility. This specific system also showcases the elegance of 'self-healing' systems where pH can easily be maintained by the reaction medium itself through an oversaturated, benign carbonate buffer reaction with product cation species.

In this work improved performance of ECS-PLE06 was achieved with final process metrics summarized in Table 2. These results point towards a promising biocatalytic reaction of up to 0.4 M (75 $g \cdot L^{-1}$) batches of product with an expected biocatalyst yield and productivity of 4.36 $g \cdot g_{biocat}^{-1}$ and 20.2 $g \cdot L^{-1} \cdot h^{-1}$, respectively. Beyond this relatively high concentration limit,

product inhibition or product induced inactivation will prevent further conversion of substrate. If higher product concentrations are required, then alternative ISPR techniques must be considered. Furthermore, substrate must be dosed in a fed-batch manner to avoid enzyme agglomeration and activity loss above 500 mM substrate.

Table 2. Process performance metrics for the ECS-PLE06-catalyzed desymmetrization of **1** to **2**.

Reaction conversion	100%
Product concentration	74 $g \cdot L^{-1}$
Space-time yield	20.2 $g \cdot L^{-1} \cdot h^{-1}$
Specific productivity	1.20 $g \cdot g_{biocat}^{-1} \cdot h^{-1}$
Biocatalyst yield	4.36 $g \cdot g_{biocat}^{-1}$

Materials and Methods

REAGENTS. All reagents were of analytical grade and supplied by Sigma-Aldrich (St. Louis, MO). Dimethyl cyclohex-4-ene-*cis*-1,2-dicarboxylate (**1**), (1*S*,2*R*)-1-(methoxycarbonyl)cyclohex-4-ene-2-carboxylic acid (**2**) and lyophilized rPLE (ECS-PLE06; EC 3.1.1.1; ≥ 0.3 $U \cdot mg^{-1}$) were kindly supplied by Enzymicals AG (Greifswald, Germany).

ACTIVITY ASSAY. The activity of pig liver esterase was quantified through spectrophotometric measurements of the degradation of *p*-nitrophenyl acetate (*p*NPA) to *p*-nitrophenolate. Reaction mixtures contained 850 µL of phosphate buffer (pH 7.5, 50 mM), 50 µL of enzyme stock solution and 100 µL of *p*NPA in DMSO (10 mM). Initial rate measurements were taken at 400 nm ($\varepsilon_{30\,°C}$ = 17759 $L \cdot mol^{-1} \cdot cm^{-1}$) over 100 s at 30 °C. One unit (U) of esterase activity was defined as the generation of 1 µmol of *p*-nitrophenolate per minute under the standard activity

assay conditions. Measurements were made using a UV-vis spectrophotometer (Specord 50, Analytik Jena AG, Jena, Germany). Reference samples contained distilled H_2O and negative controls were performed in the absence of enzyme.

SMALL-SCALE APPARATUS. Small-scale reactions were performed in a 100 mL round bottom flask using a magnetic stirrer for mixing and an external water bath for temperature control at 40 °C. 40 mL of saturated $NaHCO_3$ buffer (pH 8.15) was used to control the pH. ECS-PLE06 ($\geq$ 0.3 $U \cdot mg^{-1}$) was dosed to this medium, and the reaction was started by the addition of 0.6 g of **1** (80 mM). Samples (500 µL) were taken periodically and concentrations of **1** and **2** were determined using the procedure detailed in the analytical methods section. Reaction progress could be indirectly followed by use of a CO_2 bubble counter fixed to the top of the apparatus.

FED-BATCH 250 mL STIRRED TANK REACTOR. Fed-batch experiments were performed in a 300 mL glass jacketed stirred tank reactor (STR). 42 g of $NaHCO_3$ (corresponding to 2 M final concentration, which translates to a saturated solution with excess solid $NaHCO_3$) was added with 1500 U of ECS-PLE06 (6 $U \cdot mL^{-1}$ final concentration) to 190 mL distilled H_2O. Temperature was maintained at 40 °C by use of an external CC-K6 cryostat (Huber, Offenburg, Germany) and mixing ensured by a pitched 4-blade turbine with overhead stirring motor at 300 rpm. pH was measured by an InLab Semi-Micro electrolyte sensor (Mettler Toledo, Colombus, OH) and was found to be 8.15 ± 0.38 (mean ± SD) over all experiments using the sodium hydrogen carbonate buffered system. 60 mL of substrate **1** (corresponding to a final concentration of 1.2 M) was fed by a R99-E syringe pump (Razel Scientific Instruments, Fairfax, VT) over the first 10 hours to make up a final reaction volume of 250 mL. Triplicate samples (500 µL) were taken periodically over 24 h and concentrations of substrate and product were determined using the procedure detailed in the analytical methods section.

ANALYTICAL METHODS. Concentrations of **1** and **2** were quantified by GC-FID (TRACE 1310 Series, Thermo Fisher Scientific, Waltham, MA). Triplicate samples of 500 µL were taken from reaction media and acidified with 500 µL of concentrated HCl (1:1 volumes) to render **2** insoluble in the aqueous environment and to denature residual protein activity. Samples were then diluted and extracted with methyl *tert*-butyl ether (MTBE) containing n-decane (25 mM) as an internal standard by vortexing on the highest setting and phase separation followed by centrifugation. 1 µL of the organic phase fraction was injected into a TR-1701 column (30 m x 0.25 mm x 0.25 µm; Thermo Fisher Scientific, Waltham, MA) where the oven temperature was ramped from 130 °C to 200 °C at a rate of 5 °C min^{-1} and thereafter held at an isotherm of 200 °C for 1 min. Injector and detector temperatures were maintained at 250 °C throughout. The carrier gas flow rate was 1.2 mL min^{-1} with a split ratio of 35:1. Experimental substrate and product concentrations were determined using a standard curve generated by subjecting samples of known concentrations to the same acidification/solvent extraction procedure.

AUTHOR INFORMATION

Author Contributions

The manuscript was written through contributions of all authors. All authors have given approval to the final version of the manuscript.

Funding Sources

Funding by the German Federal Ministry of Education and Research (BMBF – Bundesministerium für Bildung und Forschung; project number: 031A123) and the German Research Foundation (DFG – Deutsche Forschungsgemeinschaft; LA 4183/1-1) is gratefully acknowledged. The

authors thank the Technical University of Denmark (DTU) for financial support for one of us (MPM).

Notes

The authors declare no competing financial interest.

ACKNOWLEDGMENT

The authors thank Prof. Dr. Udo Kragl (University of Rostock, Germany) and Prof. Dr. Uwe Bornscheuer (University of Greifswald, Germany) for their ongoing support and fruitful discussions.

REFERENCES

(1) Sheldon, R. A.; Pereira, P. C. Biocatalysis engineering: the big picture. *Chem. Soc. Rev.* **2017**, *46*, 2678-2691.

(2) Straathof, A. J. J.; Panke, S.; Schmid, A. The production of fine chemicals by biotransformations. *Curr. Opin. Biotechnol.* **2002**, *13*, 548-556.

(3) Sheldon, R. A.; Woodley, J. M. Role of biocatalysis in sustainable chemistry. *Chem. Rev.* **2018**, *118*, 801-838.

(4) Woodley, J. M. Protein engineering of enzymes for process applications. *Curr. Opin. Chem. Biol.* **2013**, *17*, 310-316.

(5) Hughes, G.; Lewis, J. C. Introduction: Biocatalysis in industry. *Chem. Rev.* **2018**, *118*, 1-3.

(6) Choi, J-.M.; Han, S-.S.; Kim, H-.S. Industrial applications of enzyme biocatalysis: Current status and future aspects. *Biotechnol. Adv.* **2015**, *33*, 1443-1454.

(7) Schmid, A.; Dordick, J. S.; Hauer, B.; Kiener, A.; Wubbolts, M.; Witholt, B. Industrial biocatalysis today and tomorrow. *Nature* **2001**, *409*, 258-268.

(8) Tufvesson, P.; Lima-Ramos, J.; Al Haque, N.; Gernaey, K. V.; Woodley, J. M. Advances in the process development of biocatalytic processes. *Org. Process Res. Dev.* **2013**, *17*, 1233-1238.

(9) Aldercreutz, P. in *Organic Synthesis with Enzymes in Non-Aqueous Media*; Wiley-VCH Verlag GmbH & Co. KGaA: Weinheim, Germany, **2008**.

(10) Meyer, H.-P.; Eichhorn, E.; Hanlon, S.; Lütz, S.; Schürmann, M.; Wohlgemuth, R.; Coppolecchia, R. The use of enzymes in organic synthesis and the life sciences: Perspectives from the Swiss Industrial Biocatalysis Consortium (SIBC). *Catal. Sci. Technol.* **2013**, *3*, 29-40.

(11) Hollmann, F.; Arends, I. W. C. E.; Buehler, K.; Schallmey, A.; Buehler, B. Enzyme-mediated oxidations for the chemist. *Green Chem.* **2011**, *13*, 226-265.

(12) Noorman, H. in *Fundamental Bioengineering*; Wiley-VCH Verlag GmbH & Co. KGaA: Weinheim, Germany, **2016**; pp. 463-498.

(13) Stocks, S. M. in *Microbial Production of Food Ingredients, Enzymes and Nutraceuticals*; Woodhead: Cambridge, **2013**; pp. 144-172.

(14) Nordblad, M.; Dias Gomes, M.; Meissner, M. P.; Ramesh, H.; Woodley, J. M. Scoping biocatalyst performance using reaction trajectory analysis. *Org. Process Res. Dev.* **2018**, *22*, 1101-1114.

(15) Duggleby, R. G. Quantitative analysis of the time courses of enzyme-catalyzed reactions. *Methods* **2001**, *24*, 168-174.

(16) Blackmond, D. G. Reaction progress kinetic analysis: A powerful methodology for mechanistic studies of complex catalytic reactions. *Angew. Chem. Int. Ed.* **2005**, *44*, 4302-4320.

(17) Duggleby, R. G. Analysis of progress curves for enzyme-catalyzed reactions: Applications to unstable enzymes, coupled reactions and transient-state kinetics. *Biochim. Biophys. Acta* **1994**, *1205*, 268-274.

(18) Süss, P.; Illner, S.; von Langermann, J.; Borchert, S.; Bornscheuer, U. T.; Wardenga, R.; Kragl, U. Scale-up of a recombinant pig liver esterase-catalyzed desymmetrization of dimethyl cyclohex-4-ene-*cis*-1,2-dicarboxylate. *Org. Process Res. Dev.* **2014**, *18*, 897-903.

(19) Wohlgemuth, R. in *Biocatalysis for Green Chemistry and Chemical Process Development*; John Wiley & Sons, Inc.: Hoboken, NJ, **2011**; pp. 277-298.

(20) Boland, W.; Niedermeyer, U.; Jaenicke, L.; Görisch, H. Enantioselective syntheses and absolute-configurations of viridiene and aucantene, 2 constituents of algae pheromone bouquets. *Helv. Chim. Acta* **1985**, *68*, 2062-2073.

(21) Yun, S. Y.; Zheng, J.-C.; Lee, D. Concise synthesis of the tricyclic core of platencin. *Angew. Chem. Int. Ed.* **2008**, *47*, 6201-6203.

(22) Andreini, M.; Doknic, D.; Sutkeviciute, I.; Reina, J. J.; Duan, J.; Chabrol, E.; Thepaut, M.; Moroni, E.; Doro, F.; Belvisi, L.; Weiser, J.; Rojo, J.; Fieschi, F.; Bernardi, A. Second

generation of fucose-based DC-SIGN ligands: Affinity improvement and specificity versus Langerin. *Org. Biomol. Chem.* **2011**, *9*, 5778-5786.

(23) Compton, T.; Gellman, S. H.; English, E. P.; Chumanov, R. S. Beta-Polypeptides that Inhibit Cytomegalovirus Infection WO2006099170, **2006**.

(24) Süss, P.; Borchert, S.; Hinze, J.; Illner, S.; von Langermann, J.; Kragl, U.; Bornscheuer, U. T.; Wardenga, R. Chemoenzymatic sequential multistep one-pot reaction for the synthesis of (1S,2R)-1-(methyoxycarbonyl)cyclohex-4-ene-2-carboxylic acid with recombinant pig liver esterase. *Org. Process Res. Dev.* **2015**, *19*, 2034-2038.

(25) Hinze, J.; Süss, P.; Strohmaier, S.; Bornscheuer, U. T.; Wardenga, R.; von Langermann, J. Recombinant pig liver esterase-catalyzed synthesis of (1S,4R)-4-hydroxy-2-cyclopentenyl acetate combined with subsequent enantioselective crystallization. *Org. Process Res. Dev.* **2016**, *20*, 1258-1264.

(26) Hülsewede, D.; Tänzler, M.; Süss, P.; Mildner, A.; Menyes, U.; von Langermann, J. Development of an in situ-product crystallization (ISPC)-concept to shift the reaction equilibria of selected amine transaminase-catalyzed reactions. *Eur. J. Org. Chem.* **2018**, *18*, 2130-2133.

(27) Bechtold, M.; Makart, S.; Heinemann, M.; Panke, S. Integrated operation of continuous chromatography and biotransformations for the generic high yield production of fine chemicals. *J. Biotechnol.* **2006**, *124*, 146-162.

(28) Meyer, L.-E.; Plasch, K.; Kragl, U.; von Langermann, J. Adsorbent-based downstream-processing of the decarboxylase-based synthesis of 2,6-dihydroxy-4-methylbenzoic acid. *Org. Process Res. Dev.* **2018**, *22*, 963-970.

(29) Strathmann, H. Electrodialysis, a mature technology with a multitude of new applications. *Desalination* **2010**, *264*, 268-288.

(30) Buque-Taboada, E. M.; Straathof, A. J. J.; Heijnen, J. J.; van der Wielen, L. A. M. *In situ* product removal using a crystallization loop in asymmetric reduction of 4-oxoisophorone by *Saccharomyces cerevisiae*. *Biotechnol. Bioeng.* **2004**, *86*, 795-800.

(31) Buque-Taboada, E. M.; Straathof, A. J. J.; Heijnen, J. J.; van der Wielen, L. A. M. *In situ* product recovery (ISPR) by crystallization: basic principles, design, and potential applications in whole-cell biocatalysis. *Appl. Microbiol. Biotechnol.* **2006**, *71*, 1-12.

(32) Wallert, S.; Drauz, K.; Grayson, I.; Gröger, H.; Dominguez de Maria, P.; Blom, C. Ionic liquids as additives in the pig liver esterase (PLE) catalysed synthesis of chiral disubstituted malonates. *Green Chem.* **2005**, *7*, 602-605.

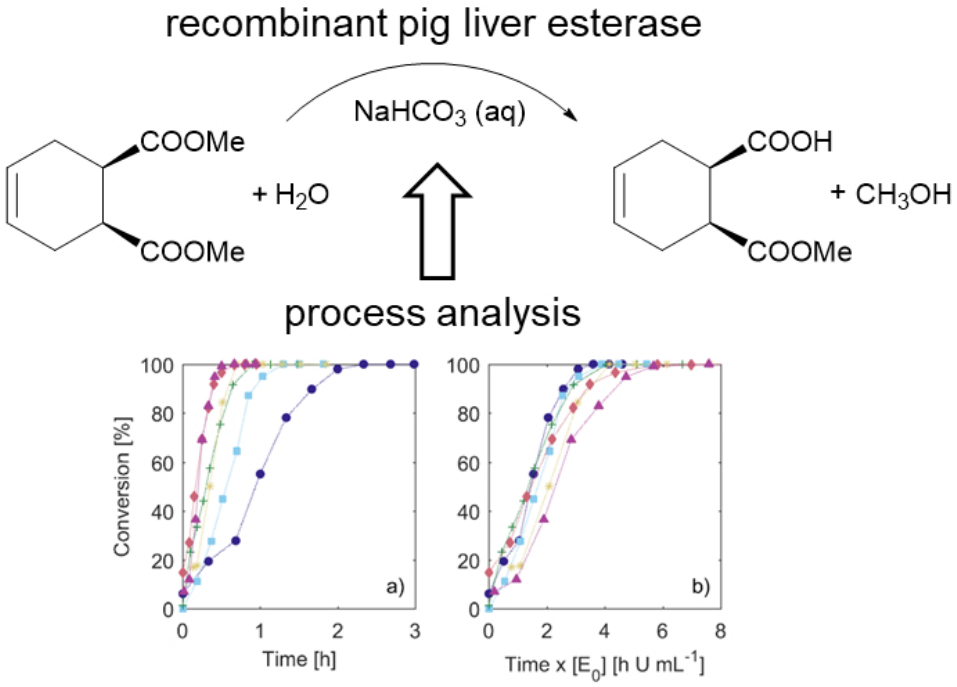

TOC-figure

61x45mm (300 x 300 DPI)